Deep learning-guided attenuation and scatter correction without using anatomical images in brain PET/MRI

Karin Bortolin, Hossein Arabi and Habib Zaidi *IEEE Fellow*

Abstract– **Attenuation correction (AC) is essential component for quantitative PET imaging. However, in PET/MR imaging and dedicated brain PET devices, the attenuation map either suffers from a number of limitations or is not readily available in the absence of CT or transmission scan. To tackle this issue, a deep convolutional neural networks is proposed to perform joint attenuation and scatter correction in the image domain on the non-attenuation corrected PET images (PET-nonAC). The deep convolutional neural network used in this work benefits from dilated convolutions and residual connections to establish an end-to-end PET attenuation correction (PET-DirAC). For the training phase, data of 30 patients who underwent brain ^{18}F-FDG PET/CT scans were used to generate reference PET-CTAC and PET-nonAC images. A five-fold cross-validation scheme was used for training/evaluation of the proposed algorithm. The quantitative accuracy of the proposed method was evaluated against the commercial segmentation-based method (2-class AC map referred to as MRAC). For quantitative analysis, tracer uptake estimated from PET-DirAC and PET-MRAC was compared to PET-CTAC. The relative SUV bias was calculated for bone, soft-tissue, air cavities and the entire head, separately. The proposed approach resulted in a mean relative absolute error (MRAE) of 4.1±7.5% and 5.8±10.4% for the entire head and bone regions, respectively. Conversely, MRAC led to a MRAE of 8.1±10.2% and 17.2±6.1% for these two regions, respectively. A mean SUV difference of 0.3±0.6 was achieved when using the direct method (DirAC) while the MRAC approach led to a mean SUV difference of -0.5±0.7. The quantitative analysis demonstrated the superior performance of the proposed deep learning-based AC approach over MRI segmentation-based method. The proposed approach seems promising to improve the quantitative accuracy of PET/MRI without the need for concurrent anatomical imaging.**

I. Introduction

ATTENUATION correction is critical for quantitative PET imaging [1]. However, accomplishing this procedure could be problematic when anatomical imaging is either not readily available as is the case on dedicated wearable brain PET devices or on hybrid PET/MRI systems where MRI-guided derivation of the attenuation map suffers from a number of issues [2]. Hence, the major challenge for these systems is the development of robust approaches for attenuation and scatter correction without relying on additional anatomical imaging [3]. In hybrid PET/MR imaging, MRI-guided attenuation correction involves the conversion of MRI into synthetic CT through bulk segmentation [4, 5], atlas-based [6] or machine learning methods [7, 8] and joint reconstruction of activity and attenuation [2]. In this work, a new approach is introduced to correct PET images for attenuation and scatter simultaneously in the image domain without using anatomical imaging. A deep learning convolutional network algorithm is employed to perform joint attenuation and scatter correction directly on PET-nonAC images. The input of this approach is PET-nonAC and attenuation correction is performed in one-phase generating PET-DirAC. For this purpose, 40 ^{18}F-FDG brain PET/CT scans were used for training and validation of the convolutional neural network through a 5-fold cross-validation scheme. PET-CTAC was considered as ground-truth for the training and validation of the network to perform joint attenuation and scatter correction on PET-nonAC. The proposed method was validated against the commercial 2-class approach implemented on the Philips Ingenuity TF PET/MR system [9].

Manuscript received December 23, 2019. This work was supported by the Swiss National Science Foundation under grant SNFN 320030-176052 and the Swiss Cancer Research Foundation under Grant KFS-3855-02-2016.

K. Bortolin, H. Arabi and H. Zaidi are with the Division of Nuclear Medicine & Molecular Imaging, Geneva University Hospital, CH-1211, Geneva, Switzerland (e-mail: habib.zaidi@hcuge.ch)

II. Material and Methods

A. Data acquisition

The study population comprised 40 patients referred to our facility for a brain ^{18}F-FDG PET/CT scan. The PET/CT scan was followed by an MRI performed on a 3T Siemens MAGNETOM Skyra using the magnetization-prepared rapid gradient-echo (MP-RAGE) sequence. PET/CT scans were performed on the Siemens Biograph 64 True Point lasting 20 min after injection of 200 ± 13 MBq of ^{18}F-FDG. CT-based attenuation correction was performed using a low-dose CT scan (120 kVp, 20 mAs).

B. Deep learning-based approach

The NiftyNet framework [10] was employed for implementation of direct attenuation correction on PET-nonAC images. NiftyNet is a modular deep convolutional learning framework, developed to facilitate the implementation of deep learning-based algorithms for a broad range of medical image analysis problems, such as segmentation, regression and data synthesis. For joint scatter and attenuation correction on PET-nonAC images, a dedicated deep convolutional neural network for regression was exploited to learn the end-to-end conversion. The employed deep learning method utilized a high-resolution compact network using dilated convolutional and residual layers [11]. In total, this network is composed of 20 convolutional layers separated into two seven- and one six-layer blocks. The first seven-layer block utilizes $3 \times 3 \times 3$ kernels intended to capture low-level features from the input image. The second seven-layer block utilizes dilated kernels by a factor of two to detect mid-level features. The last six-layer

978-1-7281-4164-0/19/$31.00 ©2019 IEEE

block uses dilated kernels by a factor of four for capturing high-level image features. Second convolutional layers are linked together by residual connections followed by a batch normalization and ReLU layer. The training was performed to minimize a loss function based on the L2 norm using Adam optimization method. The training was performed on PET images converted to SUV without any normalization factor to maintain the quantification fidelity. A 5-fold cross-validation scheme was used for the training/validation.

C. Segmentation-based 2-class attenuation map

The segmentation-based approach entails segmentation of brain MRI into 2 tissue classes including soft-tissue and background air. Internal air cavities are commonly ignored in this approach as they are filled with soft-tissue. Predefined CT values of 0 and -1000 HU were assigned to soft-tissue and background air, respectively. MRI-guided AC map obtained by this approach was used to correct the PET data for attenuation and scatter to generate PET-MRAC images.

D. Performance evaluation

PET data of each patient were reconstructed three times using CT and the MRI-guided attenuation map to generate the ground-truth PET-CTAC, PET-MRAC and without AC to create PET-nonAC. The reconstruction was performed using the Siemens VG50 e7 tool using an ordinary Poisson ordered subsets-expectation maximization (OP-OSEM) algorithm (4 iterations, 21 subsets). The relative SUV bias was calculated for bone, air cavity, soft-tissue and the entire head region separately using Eq. 1.

$$E_j = \frac{(PET_{MRAC,DirAC})_j - (PET_{CTAC})_j}{(PET_{CTAC})_j} \times 100\% \quad (1)$$

where j denotes the region (for instance bone). Moreover, the mean SUV difference was calculated between the ground-truth PET-CTAC and the two direct PET AC (PET-DirAC) and MRI-guided PET AC (PET-MRAC) approaches, separately for each of the above-mentioned brain regions.

III. Results and Discussion

Representative slices of PET images corrected for attenuation and scatter using the proposed approach (PET-DirAC) as well as the ground-truth PET-CTAC and PET-MRAC are shown in Fig. 1. The differences images obtained from subtraction of the PET-CTAC from PET-MRAC and PET-DirAC are also provided next to these two PET images.

TABLE 1. MEAN ABSOLUTE PET QUANTIFICATION ERRORS IN SOFT-TISSUE, BONE, AND AIR WITHIN THE ENTIRE HEAD CONTOUR FOR MRAC AND DIRAC METHODS WITH RESPECT TO CTAC.

	Soft-tissue mean ± SD (Abs. mean ± SD)	Bone mean ± SD (Abs. mean ± SD)	Air cavity mean ± SD (Abs. mean ± SD)	Head mean ± SD (Abs. mean ± SD)
PET-DirAC	3.8±11.4 (4.2±7.9)	1.7±11.1 (5.8±10.4)	3.1±12.2 (5.7±10.9)	3.3±2.8 (4.1±7.5)
PET-MRAC	-2.6±11.7 (7.4±9.1)	-16.8±7.7 (17.2±6.1)	40.8±10.6 (42.6±8.8)	-6.4±5.0 (8.1±10.2)

Line profiles drawn on PET images demonstrate the quantitative accuracy of the estimated activity concentration on PET-DirAC. Table 1 summarizes the relative SUV bias computed for different brain regions using MRAC and DirAC methods.

The segmentation-based AC approach tends to fill the air cavities with soft-tissue, which may result in overestimation of the activity concentration in adjacent tissues. Fig. 2 depicts an example where the miss-segmentation of the soft-tissue resulted in overestimation of activity in PET-MRAC images. The DirAC approach led to more accurate SUV estimation.

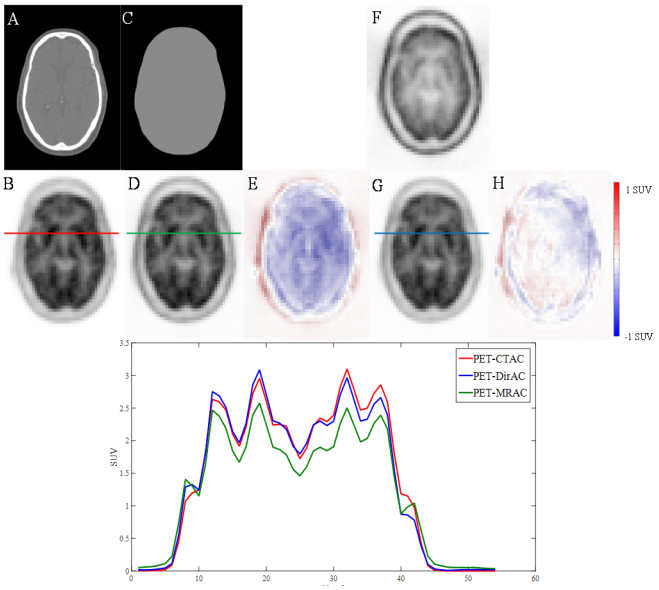

Fig. 1. A) Reference CT. B) PET-CTAC. C) 2-class AC map. D) PET-MRAC. E) PET-MRAC – PET-CTAC. F) PET-nonAC. G) PET-DirAC. H) PET-DirAC – PET-CTAC.

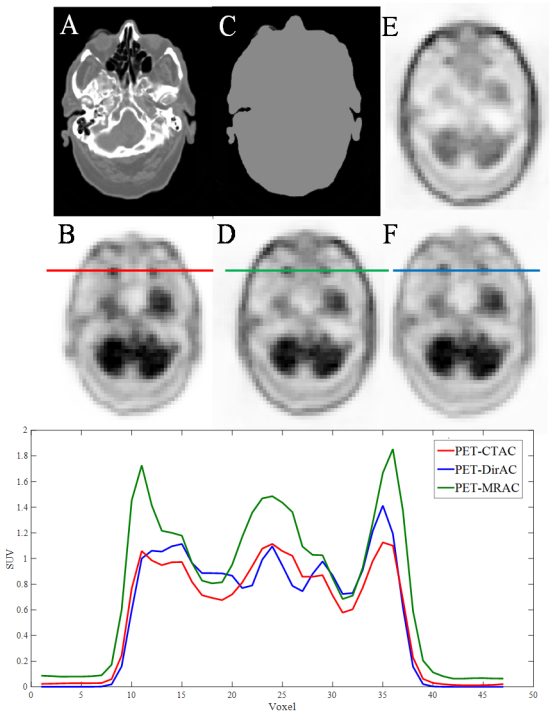

Fig. 2. A) Reference CT. B) PET CT-AC. C) 2-class AC map. D) PET-MRAC. E) PET-nonAC. F) PET-DirAC.

Table 2 summarizes mean SUV differences between PET-DirAC and PET-MRAC against the ground-truth PET-CTAC for different tissues. The quantitative analysis of PET images

demonstrated the superior performance of the proposed direct attenuation correction over the segmentation based method.

TABLE 2. MEAN SUV DIFFERENCES BETWEEN PET-DIRAC AND PET-MRAC AGAINST THE REFERENCE PET-CTAC FOR DIFFERENT TISSUES.

Mean SUV difference	**Soft-tissue**	**Bone**	**Air cavity**	**Head**
PET-DirAC	0.3±0.6	-0.1±0.5	0.2±0.7	0.3±0.6
PET-MRAC	-0.4±1.0	-0.6±0.9	0.4±1.6	-0.5±0.7

IV. CONCLUSIONS

The proposed deep learning-based scatter and attenuation correction approach of brain PET scans exhibits promising performance and eliminates the need for concurrent anatomical imaging. The quantitative PET evaluation demonstrated the superior performance of the proposed method over MRI-guided segmentation-based method.

REFERENCES

[1] A. Mehranian, H. Arabi, and H. Zaidi, "Vision 20/20: Magnetic resonance imaging-guided attenuation correction in PET/MRI: Challenges, solutions, and opportunities," *Med Phys,* vol. 43, pp. 1130-55, 2016.

[2] A. Mehranian, H. Arabi, and H. Zaidi, "Quantitative analysis of MRI-guided attenuation correction techniques in time-of-flight brain PET/MRI," *Neuroimage,* vol. 130, pp. 123-133, 2016.

[3] J. Yang, D. Park, G. T. Gullberg, and Y. Seo, "Joint correction of attenuation and scatter in image space using deep convolutional neural networks for dedicated brain (18)F-FDG PET," *Phys Med Biol,* vol. 64, p. 075019, 2019.

[4] H. Arabi, O. Rager, A. Alem, A. Varoquaux, M. Becker, and H. Zaidi, "Clinical assessment of MR-guided 3-class and 4-class attenuation correction in PET/MR," *Mol Imaging Biol,* vol. 17, pp. 264-276, 2015.

[5] H. Arabi and H. Zaidi, "Comparison of atlas-based techniques for whole-body bone segmentation," *Med Image Anal,* vol. 36, pp. 98-112, 2017.

[6] H. Arabi, N. Koutsouvelis, M. Rouzaud, R. Miralbell, and H. Zaidi, "Atlas-guided generation of pseudo-CT images for MRI-only and hybrid PET–MRI-guided radiotherapy treatment planning," *Phys Med Biol,* vol. 61, p. 6531, 2016.

[7] H. Arabi, G. Zeng, G. Zheng, and H. Zaidi, "Novel adversarial semantic structure deep learning for MRI-guided attenuation correction in brain PET/MRI," *Eur J Nucl Med Mol Imaging,* 2019, *in press*

[8] H. Arabi, J. A. Dowling, N. Burgos, X. Han, P. B. Greer, N. Koutsouvelis*, et al.*, "Comparative study of algorithms for synthetic CT generation from MRI: Consequences for MRI-guided radiation planning in the pelvic region," *Med Phys,* vol. 45, pp. 5218-5233, 2018.

[9] H. Zaidi, N. Ojha, M. Morich, J. Griesmer, Z. Hu, P. Maniawski*, et al.*, "Design and performance evaluation of a whole-body Ingenuity TF PET-MRI system.," *Phys Med Biol,* vol. 56, pp. 3091-3106, 2011.

[10] E. Gibson, W. Li, C. Sudre, L. Fidon, D. I. Shakir, G. Wang*, et al.*, "NiftyNet: a deep-learning platform for medical imaging," *Comput Methods Program Biomed,* vol. 158, pp. 113-122, 2018.

[11] W. Li, G. Wang, L. Fidon, S. Ourselin, M. J. Cardoso, and T. Vercauteren, "On the compactness, efficiency, and representation of 3D convolutional networks: brain parcellation as a pretext task," *International Conference on Information Processing in Medical Imaging*, 2017, pp. 348-360.